The Reliability Information Analysis Center (RIAC) is a DoD Information Analysis Center sponsored by the Defense Technical Information Center

JOURNAL

OF THE RELIABILITY INFORMATION ANALYSIS CENTER

FOURTH QUARTER // 2008
VOLUME 16, NO. 4

AIR FORCE C-130 RAINBOW FITTING DIAGNOSTIC TECHNOLOGY DEVELOPMENT

Jeffrey Banks, Clark Moose, Steve Conlon, and Karl Reichard,
Penn State Applied Research Laboratory
Gary Steffes, AFRL-MLLP

Introduction

The C-130 Hercules has been a workhorse for the U.S. Air Force for decades and is projected to continue to accrue flight hours for years to come as a highly capable platform utilized for numerous mission profiles. In the past few years, many C-130 aircraft have developed fatigue cracks in the center wing box rainbow fittings. These cracks can be a significant flight safety risk, when the damage is extensive. In order to detect the existence of cracks in the rainbow fittings implementation of recurring, labor intensive eddy current non-destructive inspection technology has been used. The Air Force is interested in the development and application of alternative fault detection techniques that are less time demanding to implement by the maintainers, while providing a high damage detection probability. Additionally, the future capability to embed effective rainbow fitting fault detection capability into the aircraft as an integrated systems health management (ISHM) solution is also desired.

The C-130 upper and lower rainbow fittings provide the structural connection support between the aircraft center wing box and the outer wing as shown in figure 1.

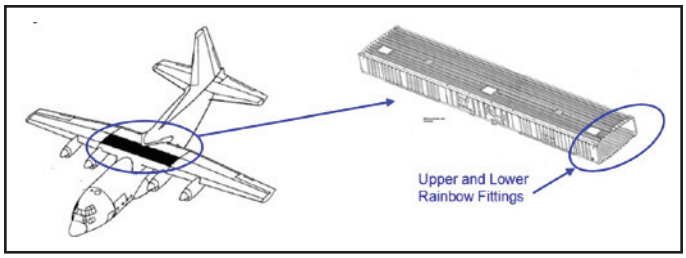

Figure 1 - C-130 Center Wing Box and Rainbow Fitting

The in-board and out-board rainbow fittings are connected by bolts that join the center wing box to the outer wing. The in-board rainbow fittings are extruded from 7075-T6 aluminum alloy and the out-board rainbow fittings are extruded from 7075-T73 aluminum alloy. The upper rainbow fitting consists of 11 pins and 10 scallops or 'rainbows' and the lower rainbow fitting consists of 13 pins and 12 rainbows as shown in figure 2.

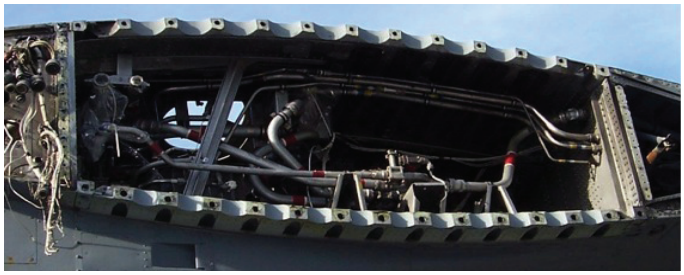

Figure 2 - C-130 Upper and Lower Rainbow Fittings

The primary cause of the cracking is from common fatigue that occurs almost exclusively on the in-board rainbow fittings. The secondary cause of cracking is from stress corrosion that occurs mainly on the in-board and occasionally on the out-board rainbow fittings [1]. The cracking occurs predominantly in the counter bore region of the fittings as shown in figure 3. A finite element analysis conducted by Lockheed Martin Aeronautics Corporation and presented in November 2006 at the USAF Aircraft Structural Integrity Program Conference indicates that the critical crack size at design limit stress is 6.5 inches [2].

Figure 3 - Picture of Typical Rainbow Fitting Cracks

The study conducted by Lockheed Martin indicates that as of January 2005, there were 44 Air Force aircraft with in-service cracking [2]. Data from the Robins AFB C-130 structures team indicates that rainbow fitting cracking has occurred on a number of aircraft including 18 upper rainbow fitting cracks on 15 aircraft and 16 lower fittings cracks on 11 aircraft.

Diagnostic Technology Background

Currently, the U.S. Air Force maintainers are using manually applied eddy current technology to provide a detection capability for rainbow fitting cracks. This technology is a widely used non-destructive inspection technique that is effective for detecting surface cracks in complex structures, but this technology is fairly labor intensive to apply, especially for structures with a relatively large surface area.

The eddy current technology is based on using two integrated electromagnetic coils built into an instrument probe. One of the coils is used to induce a magnetic field in the electrically conductive structure that is being inspected and the other coil is used to measure changes in the induced magnetic field based on the integrity of the structure. The detection capability comes from the flux lines that are created by surface cracks in the structure, which are measured by the coil in the instrument probe. The relatively small probe is uniformly moved over the surface area of the structure to scan for cracks. The probe tip must be maintained at a consistent distance from the structure to reduce variability in the measurement. The presence of a surface crack is indicated on a display that plots the inductive reactance on one axis and the resistance on the other axis as shown in figure 4.

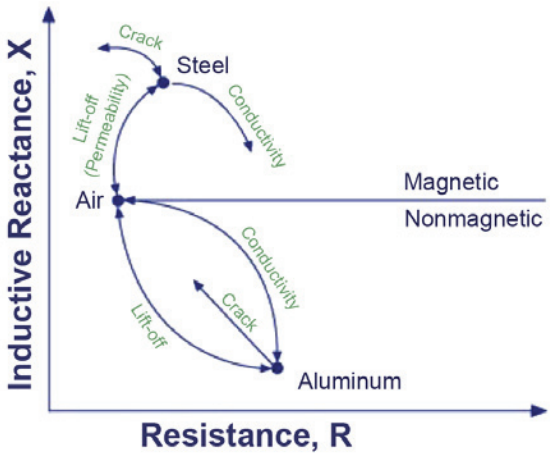

Figure 4 – Eddy Current Impedance Plane Response

If the eddy current probe is balanced in air and then located above an aluminum structure, "then the resistance component will increase (eddy currents are being generated in the aluminum and this takes energy away from the coil and this energy loss shows up as resistance) and the inductive reactance of the coil decreases (the magnetic field created by the eddy currents opposes the coil's magnetic field and the net effect is a weaker magnetic field to produce inductance)" [1]. If a crack is present in the structure then fewer eddy currents will be created and the resistance will decrease and the inductive reactance will increase.

The ability to reliably detect cracks in relatively large and geometrically complex structures such as the C-130 rainbow fitting is dependant on the training, testing experience as well as the ability of the inspector to focus for significant lengths of time on the impedance display, which requires continuous concentration to interpret the results. Due to the probability of a high rate of missed detections for this application, the Air Force is interested in an alternative inspection technique that is less labor intensive to implement and provides a high probability of detection, fault isolation and some degree of fault severity indication.

Acoustic Emission Technology

After a preliminary cursory evaluation of several technologies including ultrasound and natural frequency assessment, the primary technology that was chosen to provide crack detection and fault isolation is Acoustic Emission (AE). AE is a non-destructive evaluation technique that is used for surface and inner structure crack detection and localization. This technology involves monitoring for the emission of high frequency vibration (> 100,000 Hz) as an existing structural defect (crack) is stressed from the static loading of the system. An analogous low frequency example of this technique is when a tree branch is strained from a hung weight; the branch emits an audible cracking sound. The source of this audible sound (20 – 18,000 Hz) is from the load induced strain of a defect or crack that exists in the branch. The audible sound provides the indication that the crack exists. The application of the load is one of the most critical aspects of this technique. If sufficient load is not applied during testing, then a material strain with corresponding acoustic emission indication will not be induced. If too much load is applied,

continued on next page ›››

continued from page 3

then the existing crack could be significantly propagated and the severity of the defect could be detrimentally increased.

There are several advantages to the application this technology. The primary advantage is that since this a high frequency (100,000 to 1,000,000 Hz) technique there is inherent better signal to noise ratio (SNR) capability. Since most of the standard machinery and electrical noise sources (i.e. gears vibration, engine vibration, AC motor pulse width modulation (PWM), etc.) occur below 100,000 Hz with most of the noise concentrated below 20,000 Hz; at frequencies above 100,000 Hz the noise floor is relatively low. With a low noise floor at higher frequencies, even low amplitude 'acoustic emission' vibration can be easily detected because of the high SNR. SNR is a significant factor affecting detectability of a fault at the earliest time in the fault propagation evolution, which provided the longest lead time for managing the correction of the fault. Another advantage is once the technology has been developed and validated, the technique has the ability to quickly isolate the fault location within the structure. This capability will facilitate additional detailed inspection (i.e. eddy current, visual, etc.), which reduces the amount of time to confirm the extent of the damage and the need for extraction of the damaged structure. The final significant advantage related to this technology is that it lends itself well as an embedded diagnostic solution that can gather data during flight operations. Since rainbow fitting loading is required to induce an acoustic emission for fault detection and isolation, this loading will be implemented during aircraft take off, high g maneuvers and landing. The hardware does not require a tremendous amount of power and the sensors and hardware are compact enough that they can be readily integrated into the aircraft. As an embedded solution, each aircraft could be constantly monitored during operations with an early indication of a fault being provided to maintenance after each flight and an indication provided to the fight crew during operations if required.

Laboratory Testing

The first step in the process of evaluating the effectiveness of acoustic emission technology to detect and isolate cracks in rainbow fitting structures was to conduct component level tests on undamaged rainbow fittings in the laboratory. Due to the limitation that the structure could not be loaded in the laboratory, two objectives were developed. The purpose of the first test was to evaluate the vibration transmissibility through the rainbow fitting. This evaluation can provide an indication of the ability for the interrogation frequencies that are used for the AE technology (> 100,000 Hz) to propagate through the length of the structure. The purpose of the second laboratory test was to evaluate the localization of an impulse event applied to the structure. This assessment provided an indication of the ability to detect and locate a simulated crack emission event.

The first test was conducted on an undamaged upper rainbow fitting with a short length of hat stiffeners attached.

In order to conduct the laboratory testing for evaluating vibration transmission through the structure, three sensors were positioned along the length of the upper rainbow fitting, one at the middle and one at each end of the fitting. Since the test specimen does not have a fault, we are unable to initiate an acoustic emission from a crack from applied loading. In order to provide an acoustic signature, a piece of 0.5 mm mechanical pencil lead was applied at the bolt locations to initiate an acoustic event. The lead was applied to the fitting with enough force to break the lead, which caused vibration waves to travel through the structure. This technique is based on the American Society for Testing and Materials (ASTM) standard method (E 976-94) for conducting pencil lead break tests for AE sensors. The lead break technique was applied at multiple locations from end to end along the fitting.

The results of this test sequence indicate that acoustic emission energy propagates along the length of the rainbow fitting without significant signal attenuation. The complex structural geometry does not appear to have any significant effect on signal strength. The data in figure 5 illustrates the signal strength to each sensor as a function of position along the fitting.

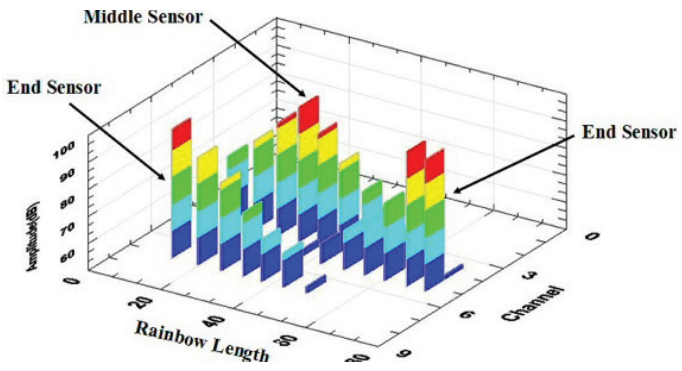

Figure 5 - Signal Response as a Function of Position along the Rainbow Fitting

Based on the signal strength from this preliminary analysis, it was determined that four sensors should be sufficient for source localization. It may be determined that more sensors are needed for crack isolation when testing is conducted on a rainbow fitting attached to the aircraft. This is because the signal attenuation should increase because of the increased mechanical coupling with the aircraft structure that provides more vibration paths

through which the energy would dissipate between the source and the sensor locations.

In order to determine the location of a crack or discontinuity (i.e. source location), the distance between sensors and the time of travel of the vibration waves must be measured and the wave velocity of the material must be calculated. The source location is determined by first measuring the time delay between two sensors (Time 2 – Time 1) when an impulse is applied to the structure as shown in figure 6.

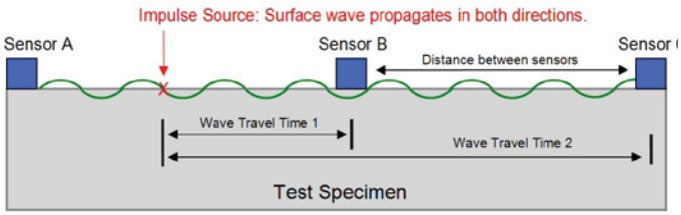

Figure 6 - Diagram of Parameters for Calculation of Wave Velocity

The wave velocity can be computed by measuring the distance between two sensors (i.e. Sensor B and Sensor C) and the time delay between the sensors as shown in equation 1.

$$\text{Wave Velocity} = \text{Distance}/(\text{Time 2} - \text{Time 1}) \quad (1)$$

With the wave velocity and time of travel for each sensor, the distance from the sensors to the source of the vibration energy can be calculated as shown in equation 2.

$$\text{Distance (Sensor B to Source)} = \text{Time1} \times \text{Wave Vel.} \quad (2)$$

The second laboratory test was conducted to evaluation the use of acoustic emission for fault localization. This test was conducted on the lower rainbow fitting. Four AE sensors were positioned along the length and their exact separation measured as shown in figure 7.

At each of the 13 bolt holes indicated, four lead breaks were initiated around the hole perimeter. The calculated positions of the four lead breaks per hole (acoustic events) is shown in figure 8. The position of the sensors is shown along the top of the graph with the dimensions in inches along the bottom. The thirteen hole locations are clearly determined by the grouping of the AE events.

The laboratory testing at ARL has determined that there is excellent vibration transmission through the rainbow fittings extracted from the aircraft as an individual component. It also shows that there is an accurate capability to localize acoustic events in the test specimen with 4 sensors for fault isolation.

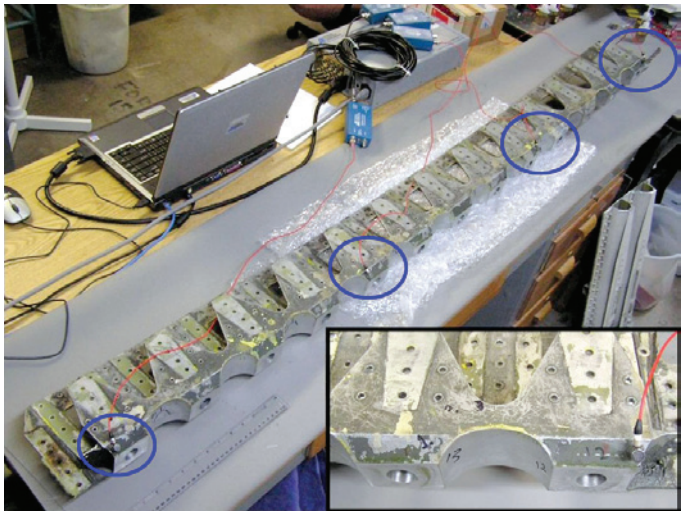

Figure 7 - AE Source Location Testing with Close-Up of Sensor Position

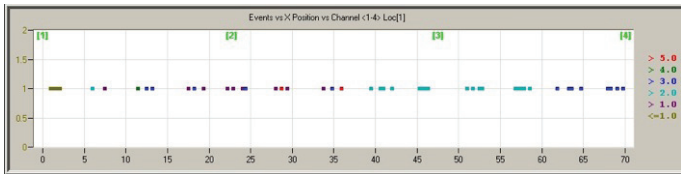

Figure 8 - AE Source Position Results with all Thirteen Holes Identified

Field Testing

The next step in the technology development and evaluation process was to conduct testing on an operational aircraft with a known rainbow fitting crack. Based on the results of the laboratory testing, a test plan and survey procedure was developed for testing on an operational C-130 aircraft. The most significant field testing issue related to testing on a full size aircraft was determining how to effectively load the wing to provide an acoustic signature from the cracked rainbow fitting. Taking into account Air Force maintenance procedures, testing requirements and the geometry of the structure, it was determined that two test procedures would be implemented in order to provide a sufficient load to both the upper and lower rainbow fittings. The first procedure was implemented by jacking the wings upward to a static no load position. This procedure would generally remove the compressive force applied to the lower rainbow fitting and remove the tensile force applied to the upper rainbow fitting due to the weight of the wings. The second procedure was implemented by adding fuel to the wing tanks and the external fuel tanks. This procedure would generally apply a compressive

continued on next page ›››

continued from page 5

force to the lower rainbow fitting and a tensile force to the upper rainbow fitting from the weight of the fuel loaded wings.

An aircraft with a known rainbow fitting crack was identified and made available for testing from July 31 – August 1, 2007 at the Little Rock Air Force Base. The crack was located in the upper right rainbow fitting on the fourth bolt connection point as shown in figures 9 and 10.

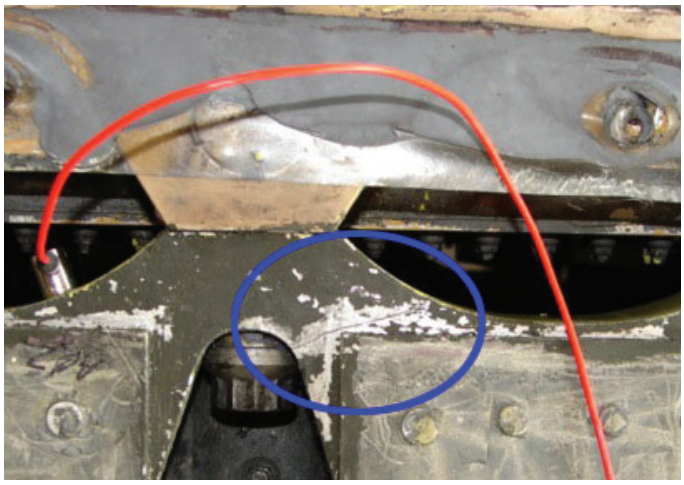

Figure 9 – Crack Location on Upper Right Rainbow Fitting

Based on the fault location and the number of channels for the data acquisition system, it was determined that just the upper left and upper right rainbow fittings would be instrumented and tested as shown in figure 10.

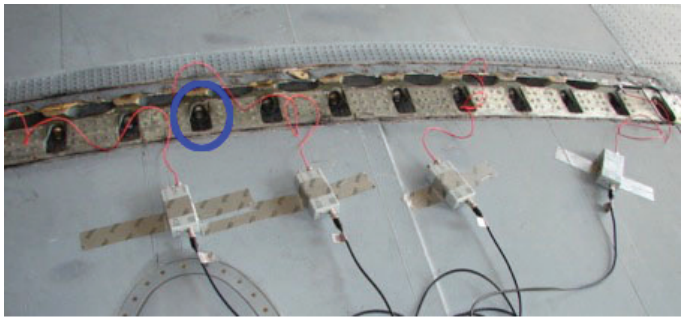

Figure 10 – Transducer Configuration for Field Test

Four transducers per upper rainbow fitting were applied, which provides the ability to sufficiently monitor each fitting based on the laboratory results and compare the acoustic emission results of the upper right 'cracked' fitting to an identical upper left 'uncracked' fitting that encounters the same loads during the tests. The comparison between the left and right fittings provides a reference for evaluating how much energy is emitted from a wing with a cracked fitting compared to a wing without a known cracked fitting. Due to the limited amount of time available to conduct the tests and the lack of existence of a known crack on the lower rainbow fittings, the lower fittings were not instrumented and tested.

The first test consisted of gathering acoustic emission data during the implementation of the standard wing 'no-load' jacking procedure. This procedure basically involves placing hydraulic jack stands outside the number one and four engines and lifting the wings until they reach a no-load position. The results of the AE test from the upper right rainbow fitting are shown in figure 11.

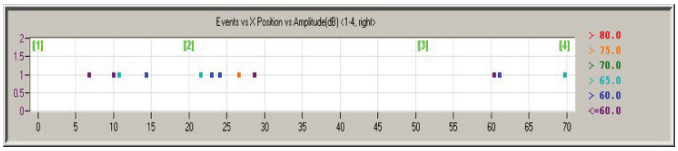

Figure 11 – Results of AE Wing Unload Test

The plot shows the length of the rainbow fitting on the x-axis in inches (70 inches) as well as the location of the four AE transducers by the numerical indications at the top of the plot. The data in the plot indicates the detection of multiple acoustic events that exceeded the defined threshold level during the test. The threshold was set for a very low level to accept most incidents during the test. The AE amplitude level provides a relative indication of the AE event magnitude and is shown by the color code indications on the right side of the plot. The location of the AE event along the length (front to back of the wing) and width (left to right of the aircraft) of the rainbow fitting is shown on the x-axis and y-axis, respectively. Since the sensor array consists of a one dimensional array, the y axis indications are all in the same plane. The data results show several events between transducers 1 and 2, several events to the right of transducer 2 (towards the back of the wing), two events between transducer 3 and 4, and one event on transducer 4. The amplitude indication from the color code shows that the only significant event occurs to the right of transducer 2, in proximity to the fault. The small inaccuracy in the event location relative to the true fault location is related to the limited number of sensors and the indirect vibration wave path from the fault to the transducers due to the complex geometry of the fitting. This single test provides a positive indication of the fault's existence and a fairly accurate location of the crack. In order to increase the effectiveness of the technology, a more optimum threshold can be determined and implemented to filter out events not related to faults.

When subsequent no load tests were conducted, the signature from the crack was significantly lower. The survey team

evaluated the cause of the crack emission during the unload procedure, and it was postulated that small particles of material debris located in the crack were compressed during the unload process, which provided the event emission. Though this was not necessarily expected, this occurrence provides a positive indication event for fault detection and localization.

The second test consisted of gathering acoustic emission data during the implementation of the aircraft fueling procedure. The procedure consisted of adding a total of 36,000 lbs of fuel in the following sequence: fuel was first added to the number 1 and 4 internal wing tanks, then to the number 2 and 3 internal wing tanks and then to the external tanks that hang under the wings. The results from the upper right rainbow fitting are shown in figure 12.

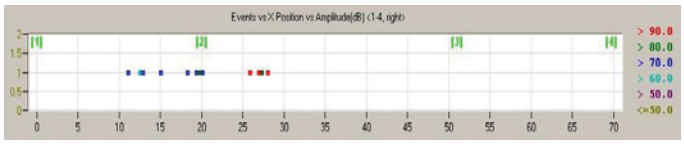

Figure 12 – Results of AE Fuel Loading Test

The high amplitude events shown on the plot between location 25 and 30, coincide well with the location of the crack in the right upper rainbow fitting. These emissions had the highest magnitude events during the test. Several additional low amplitude AE events were detected at the number two bolt location and at wing positions 10 to 15.

A cursory eddy current inspection after the testing was completed did not provide an indication of cracks in these locations. The Air Force is planning on removing and replacing the rainbow fittings on the test aircraft. The fittings will be sent to ARL Penn State for further inspection. The objective is to correlate the field AE results to any cracks that exist but were not identified previously. So the significance of these events will not be known until after the rainbow fitting is removed and examined.

Conclusions

The Air Force has a significant need for the development and application of a non-destructive inspection technology for the evaluation of C-130 rainbow fittings. Though the eddy current technology is effective for the detection of large cracks in accessible areas of the fitting or when the inspection is limited to a small region of the fitting. This technology is not the optimum approach for regular inspections of a large number of aircraft with the objective of having a high probability of detections for cracks of a certain length.

Based on the testing conducted at the component level in the laboratory and at the aircraft level in a field environment, the acoustic emission technology has demonstrated in that it can provide a less labor intensive and possible higher probability of detection capability than eddy current technology. Before this technology can be widely utilized and implemented further testing must be conducted to evaluate several factors including: the determination of the probability of detection, evaluation of the sources of false positives and optimization and formalization of the load application procedure.

The AE technology has the potential to be further developed and applied as an ISHM capability that would provide a regular assessment of rainbow fitting integrity and crack propagation. The C-130 aircraft will continue to be utilized by the Air Force for a decade or more, so the need for reliable and accurate inspection and health assessment technologies will become even more necessary in the years to come.

Acknowledgements

This work is supported by the Air Force Research Laboratory under subcontract number 06-S508-009-09-C1 through UTC. The content of the information does not necessarily reflect the position or policy of the Government, and no official endorsement should be inferred.

The principal investigator for this project was **Jeffrey Banks** who can reached at 814-863-3859 or jcb242@psu.edu.

References

1. Warner Robins-ALC/ENFM, Flight/Mechanical Systems Division, Technology and Engineering Directorate, 'Failure Analysis of a Lower Center Wing Joint Fitting From an MC-130H Aircraft', Report Number: 04-MFA-026, File Number: C130-612, September 28, 2004
2. P. Christiansen; G.R. Bateman; A. Navarrete; 'C-130 Center Wing MSD/MED Risk Analysis', 2006 USAF Aircraft Structural Integrity Program Conference, November 28, 2006
3. American Society for Testing and Materials, 'Standard Guide for Determining the Reproducibility of Acoustic Emission Sensor Response', E 976-94, 1998.
4. Peter J. Schull; Nondestructive Evaluation: Theory, Techniques and Applications, Marcel Dekker, Inc., 2002

CUSTOMER-FACING RELIABILITY GROWTH MODELING TO IMPROVE CUSTOMER SATISFACTION (PART 1 OF 2)

Bill Lycette, Agilent Technologies

Design ruggedization is a necessary step in the development of new products to ensure high reliability and high levels of customer satisfaction. It makes good business sense to have a rich understanding of whether or not the project team is on track towards achieving the project's reliability goals. Should a project fall behind in attaining these goals, it behooves the business to implement mitigation strategies as early as possible. Most design ruggedization and Design for Reliability tools do not provide system-level predictions of fielded reliability. What is needed is a tool for predicting expected customer-experienced reliability during the product development phase, and this is where reliability growth analysis can help.

Reliability growth analysis is a set of mathematical tools that provides the capability to predict fielded reliability. But effective reliability growth modeling is more than just mathematical and statistical procedures; it also encompasses processes for data collection, failure counting, effectiveness factor assignment and transformation of reliability growth results into expected customer experiences.

This article explores the practical aspects of customer-facing reliability growth analysis. Through a combination of theory and application, practical solutions for overcoming reliability growth obstacles are presented.

In Part 1 of the article, limitations of design ruggedization and Design for Reliability are discussed. Reliability growth analysis is introduced as a solution for the early prediction of fielded reliability. Processes for collecting on-time data, defining what failures should count, and rigorously calculating BD mode effectiveness factors are discussed.

In Part 2 of the article, Agilent's customer-facing reliability growth process is applied to three new product introductions. Results of the reliability growth models are discussed and methods for transforming Projected MTBF's into accurate customer-experienced reliability metrics are presented.

Introduction

Successful new product introductions typically include a battery of reliability tests intended to meet design ruggedization and qualification requirements. However most of these tests are not intended to predict fielded reliability. Project cost constraints and time-to-market pressures often times rule out the type of demonstration testing necessary to make accurate fielded reliability predictions. Still, it is highly desirable to have a richer understanding of how the product is likely to behave in reliability terms before the product is released to customers. What is needed is a customer-facing reliability prediction tool that provides reasonable accuracy at affordable investments in time and material. Reliability growth modeling can provide such insights.

Reliability growth modeling is hard work and fraught with obstacles. Successful reliability growth modeling relies on a combination of complex mathematics, data collection and handling methods, process rigor, analysis, experience, diplomacy and salesmanship. However, the potential payoff is big: a rich understanding of the reliability of a new product before it is released to your customers. These early insights are valuable in developing mitigation strategies to improve customer experiences with newly-released products.

This article describes the application of reliability growth methods on complex electronic measurement systems based on the collective experiences gained over three R&D projects. From practical experience and empirical learnings, a reliability growth modeling process has been created and refined so that useful predictive results can be realized.

Background

Agilent Technologies designs, manufactures and markets Test & Measurement equipment serving customers in more than 100 countries. With a heritage dating back 70 years when Hewlett-Packard was founded, Agilent is a leader in the Electronic Measurement and Bio-Analytical Measurement businesses.

The article focuses on reliability growth modeling applied to RF/microwave test and measurement equipment. These products include complex measurement systems such as spectrum analyzers, microwave sources, network analyzers and RF communication testers. Key assemblies used in the construction of

these products include high frequency printed circuit assemblies, hybrid microcircuits, electromechanical assemblies, precision mechanical parts, power supplies, CPU's, displays, hard drives and high performance cabling.

Much of the business is characterized by low volume/high mix products. Complexity ranges from system part counts of several hundred components to more than 20,000 components. Since prototype units can each cost between $10k-$50k and more, their scarcity makes implementation of traditional Design for Reliability (DfR) processes a challenge.

Design Ruggedization and the Case for a New Game Plan

Much has been written about the high cost of correcting design errors and weaknesses late in the design cycle and early manufacturing stages. The literature suggests mistakes corrected on pilot units cost 10X more than correcting them on prototype units, and 100x more if corrected in production.

Design ruggedization is all about discovering design weaknesses and errors early in the product life cycle in order to avoid costly fixes later. There are numerous design ruggedization tools and processes available to reliability engineers. Processes for de-risking component selection and de-rating component stress levels are helpful at the device level. Thermography tools such as the IR camera are effective in verifying stress de-rating. Margin testing, step-stress testing and HALT testing are useful for uncovering weakest links in the design.

These processes are effective design ruggedization techniques, but they are not intended to predict eventual reliability of fielded products. Accelerated Life Testing (ALT) can provide insights into expected reliability at the component and subassembly levels, but ALT is often times not practical or feasible at the system level. Part count and part stress analyzer methods such as MIL-HDBK-217 are intended to provide estimates of system-level reliability, however problems associated with inaccurate stress level assumptions and missing data associated with custom parts can lead to poor predictive results.

What is needed are tools that provide accurate prediction of eventual fielded reliability so that informed technical and business decisions can be made during the product development cycle. Reliability growth analysis on prototypes and pilot units can provide such early insights into the understanding of how the product will perform in the field, and can enable New Product Introduction (NPI) project managers to make more informed business decisions.

NPI prototype and pilot units are sent through a battery of DfR and design ruggedization tests. Most DfR plans look great on paper before the first prototype is built and the first test is conducted. As the NPI progresses, the reality of an imperfect and challenging DfR world creeps in as the competing project pressures of cost, schedule and scope present themselves. With a few previously noted exceptions, most DfR tools, processes and tests do not predict field failure rates. Consequently, customers can unintentionally become participants in the process of verifying the effectiveness of DfR and design ruggedization programs. Exacerbating this problem is the fact that most traditional reliability metrics (e.g. warranty fail rates) can take several months before it becomes clear if the NPI's reliability goals have been achieved [Reference 1].

Reliability Growth Analysis

Customer-facing reliability growth analysis (RGA) is a structured set of data collection procedures and mathematical techniques for measuring reliability maturity (growth) with the objective of ultimately predicting customer-experienced reliability before the product is released [Reference 2].

The premise of reliability growth (RG) is that a product's reliability improves as latent failure modes are discovered and failure intensity is reduced. The rate of RG improvement is proportional to the rate of occurrence of these failure modes. Improvement in Projected MTBF via failure mode discovery and corrective action can be calculated using mathematical models and statistical methods [Reference 3].

Agilent utilizes the Crow Extended Model for RGA. This model provides for the calculation of Demonstrated and Projected reli-

continued on next page ›››

continued from page 9

ability [Reference 4]. Using failure mode nomenclature from this model we have:

A modes:	No corrective action planned.
BC modes:	Corrective action taken during the test.
BD modes:	Corrective action delayed until after the completion of the current test; Effectiveness Factor (EF) assigned to future corrective action.

Collectively, A modes and BC modes represent Demonstrated reliability. In the Crow Extended model, the addition of BD modes enables for the calculation of Projected reliability.

The system failure intensity is represented by a Non-Homogeneous Poisson Process (NHPP) and the resulting modeled data is fitted to mathematical expressions such as the Weibull, Power Law or Loglinear functions.

The NHPP system failure intensity is given by

$$u(t) = \lambda\beta t^{\beta-1}$$

where β is the shape parameter. When $\beta > 1$, the time beween system failures is decreasing which indiates negative reliability growth. When $\beta < 1$, the time between system failures is increasing which indicates positive reliability growth. When $\beta = 1$, the time between system failures is constant (no reliablity growth) and the expression for system failure intensity reduces to the Homogeneous Poisson Process (HPP) with $u(t) = \lambda$ [Reference 5].

The projected failure intensity λ is given by

$$\lambda = \lambda_{dem} - \lambda_{BD} + \sum_{i=1}^{n}(1 - EF_i)\cdot\lambda_i + \overline{EF}\cdot h(t)$$

where

λ_{dem} = demonstrated failure intensity before implementation of delayed fixes
λ_{BD} = failure intensity of BD modes
EF_i = effectiveness factor of the i^{th} BD mode fix
λ_i = failure intensity of the i^{th} BD mode
$\overline{EF}$ = average effectiveness factor of BD mode fixes
h(t) = rate of occurrence of unique BD modes

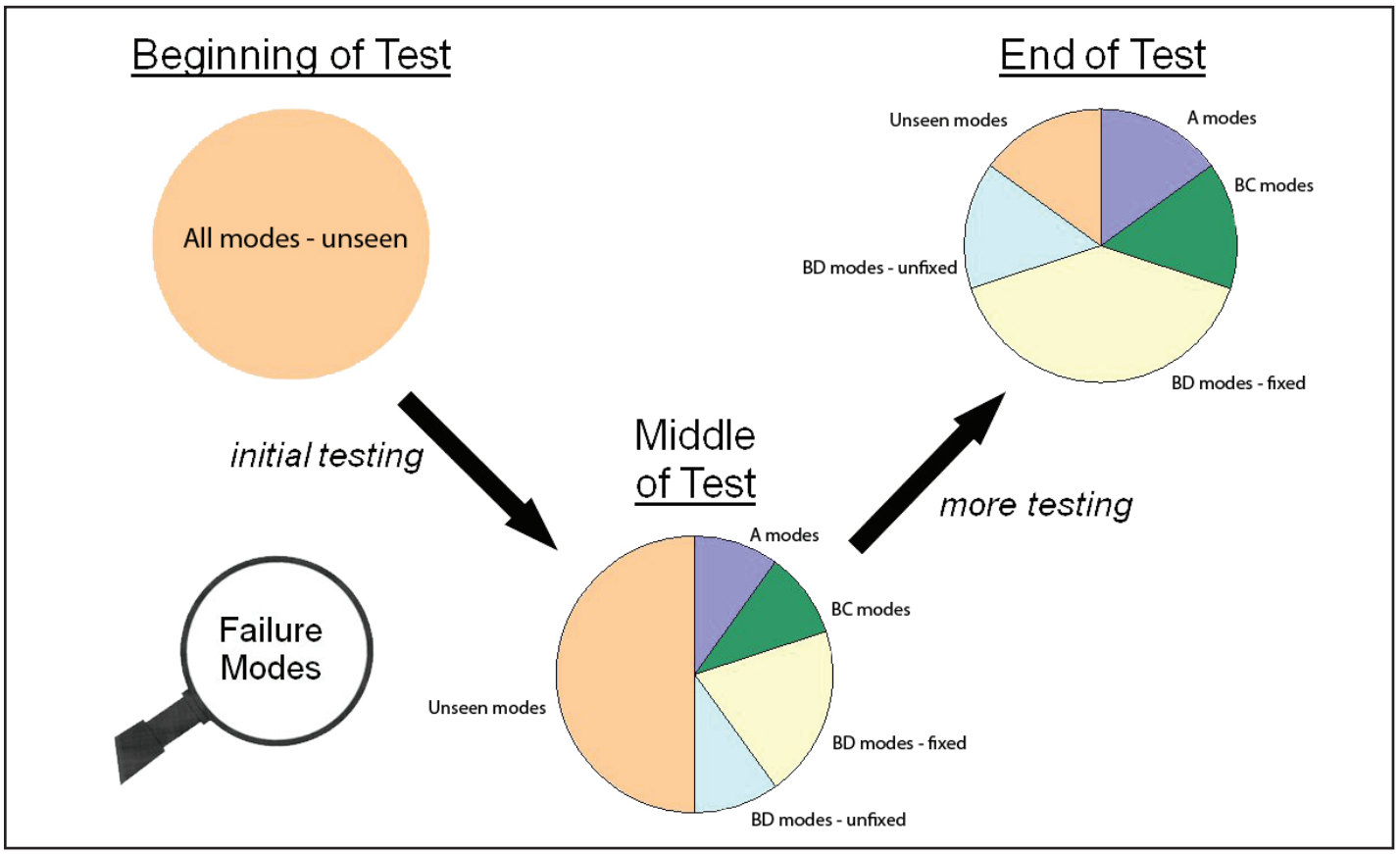

Figure 1. Reliability Growth: discovering latent failure mechanisms and converting them to BC modes and BD modes.

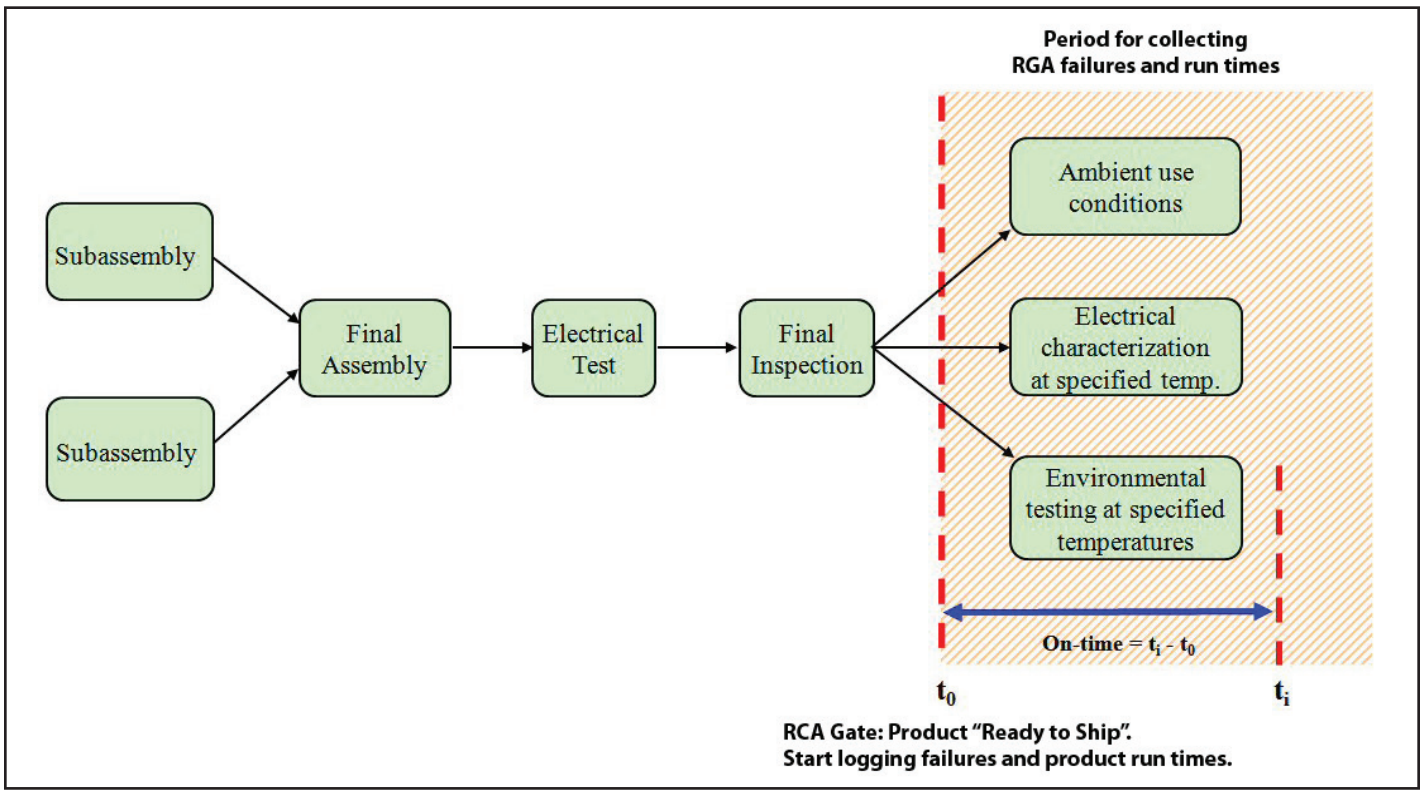

Figure 2. RGA Gate: determining when failures should start being counted.

It is instructive to understand the components of this equation and their role in affecting reliability growth [Reference 6].

λ_{dem}	Demonstrated failure intensity, no delayed fixes (A modes and BC modes)
λ_{BD}	Remove failure intensity of BD modes (delayed fixes at 100% EF)
$\sum_{i=1}^{n}(1-EF_i)\cdot\lambda_i$	Add back in delayed fixes on BD modes that didn't work
$\overline{EF}\cdot h(t)$	Unseen failure modes

Reliability growth involves detection of latent failure modes and taking corrective action to eliminate them. The role of the reliability engineer is to discover these failure modes as quickly as possible and drive corrective action. The RG process described here relies primarily on ambient use conditions to identity latent weaknesses and defects. Accelerated stress conditions (e.g. vibration and humidity testing) are avoided because of difficulties in accurately calculating acceleration factors. Figure 1 shows the concept of what we are trying to achieve with RGA. We want to convert latent unseen modes to BC modes and BD modes, we want to do this as quickly as possible, and we want to implement corrective actions that are as robust and effective as possible.

The Agilent RGA Process

Elements of Agilent's RGA process include collection of hardware failure data, collection of product on-time hours, assignment of BD mode effectiveness factors, interpreting RG model results and communicating those results in company-recognizable terms.

Collecting Hardware Failure Data

As the process is meant to be a "customer-facing" RG model, failures are only counted *after* the product has been fully assembled and verified to be functioning properly. Figure 2 shows the "RGA Gate."

Deciding what failures should count and which ones should be excluded can be a tricky and contentious affair. These decisions often times involve engineering judgment and are best made by a team consisting of cross-organizational members.

continued on next page ›››

continued from page 11

Guiding principles in these decisions should be consistent with the overall objective of measuring customer-facing RG on the design, mature supply chain and mature manufacturing processes.

- Only count failures *after* the system has successfully completed performance testing and has been deemed fit for customer use.
- Some of the testing will be on units where final specs have not yet been set. For spec-related issues, use engineering judgment and log defects where the product's performance would likely have failed what is believed to be the final specs.
- Only count failures where there is a high probability that a customer would observe the fault.
- Count failures observed under normal ambient use conditions and brief operation at spec'd cold and hot temperature.
- Count all design-related failures except for defects where the affected functionality was not intended to be available at that moment in time.
- Count mature process failures.
- Count mature component failures caused by defective material.
- Do not count failures caused by highly-accelerated stress conditions, including mechanical shock and random vibration, humidity and step-stress/HALT testing.

Collecting Run Time Data

In addition to collecting failure details, creating an RG model requires that the cumulative product on-time hours are tracked during test and ambient use. In order of preferred on-time data collection methods, the options include:

1. automated on-time clock queries;
2. periodic inventory of on-time hours and interpolation for RG modeling purposes; and
3. use of estimated average daily number of on-time hours.

Resetting the product's internal clock should be avoided if possible as this can lead to confusion and errors.

Assigning BD Mode Effectiveness Factors

In the Crow Extended model, each BD mode (delayed corrective action) requires the assignment of a corrective action Effectiveness Factor (EF). The purpose of the BD mode EF is to estimate the fractional decrease in failure intensity that is expected to occur as a result of the future corrective action. Effectiveness Factors range in value from 0.01 to 0.99. The literature suggests the average EF for a corrective action is 0.7. This figure is based on empirical results obtained from numerous government and industry RG models. However it would be helpful to have a more rigorous process to assign EF's rather than using an average 0.7 number or assigning EF's based on "gut feel."

A more robust EF procedure was established to provide greater rigor in assigning EF's. Three factors are considered in the EF calculation: 1) depth at which root cause was understood, 2) certainty that root cause was removed, and 3) degree to which measures have been put in place to prevent reoccurrences. Table I shows an example of how these factors are utilized to arrive at an overall EF for a given BD failure mode.

	Understanding Root Cause		Certanty of Removal		Prevention Copntrol		Effectiveness Factor
High	.36	Full understanding of root cause	.3	Change in design, part, or process	.3	Design or process controls prevent unapproved changes	
Meium	.3	Root cause hypothesized but not 100% confirmed	.2	Date code purge; process change by supplier.	.15	Reliance on undocumented processes to maintain fix.	
Low	.15	Failures may still occur, but symptoms characterized and screening process will be used.	.1	Supplier could not confirm failure mode.	.1	Control based on assumption and good intentions	
Score	.3	+	.3	+	.3	=	.9

Table I. Methodology for calculating Effectiveness Factors.

In this example, Root Cause was hypothesized with high confidence but not absolutely confirmed, thus 0.3 EF points were granted. In reviewing the corrective action, Certainty of Removal was judged to be high in this case and 0.3 EF points were awarded. The third EF factor is Prevention Controls such as those by provided by Six Sigma methods. In this example a new set of poke-yoke tools were implemented so 0.3 EF points were given. The total EF assigned to this BD failure mode is determined by summing up the three EF components to arrive at an Effectiveness Factor of 0.9. (Note: the High/Medium/Low weighting factors shown in the table have been modified to protect proprietary information.)

In Part 2 of this article (to be published in the First Quarter 2009 RIAC Journal), elements of the customer-facing reliability growth modeling process are applied to three NPI's. Results of the models are discussed and a method for converting the models' Projected MTBF's into customer-experienced first year failure rates is presented.

References

1. "The iFR Method for Early Prediction of Annualized Failure Rates in Fielded Products", Bill Lycette, SRC Journal – 2006 Quarter 1, http://src.alionscience.com/pdf/1Q2006.pdf
2. NIST/SEMATECH e-Handbook of Statistical Methods, Chapter 8.1.9 "How can you model reliability growth?" http://www.itl.nist.gov/div898/handbook/apr/section1/apr19.htm
3. Sample Reliability Growth Analysis cases studies compiled by ReliaSoft Corporation, http://www.reliasoft.com/RG//examples/index.htm
4. "An Extended Reliability Growth Model for Managing and Assessing Corrective Actions" presented by Dr. Larry Crow at the 2004 Reliability and Maintainability Symposium, Los Angeles, CA, http://www.reliasoft.com/pubs/2004rm_06B_01.pdf
5. "Case Study: Reliability Models and Misconceptions", John S. Usher, Quality Engineering, Volume 6, Issue 2, pp 261- 271 (October 1993).
6. "Reliability Growth Applications and Advancements" by David E. Mortin, Ph.D. and Stephen P. Yuhas, 19 November 2001, U.S. Army Test and Evaluation Command, http://www.ndia.org/Content/ContentGroups/Industrial_Working_Groups/Industrial_Committee_on_Operational_Test_and_Evaluation/PDFs22/Mortin-Yuhas.pdf

Harness the Power of Reliability

Building Reliable Products Begins with Relex®

Relex Reliability Studio

- Fault Tree/Event Tree
- FMEA
- FRACAS
- Human Factors Risk Analysis
- Life Cycle Cost
- Maintainability
- Markov
- Optimization and Simulation
- Reliability Block Diagram
- Reliability Prediction
- Weibull

Gaining and maintaining your customers' trust is critical in today's competitive, global marketplace. That trust is built by consistently providing the reliable, quality products that your customers depend on.

That's where Relex can help. Relex has the tools you need to meet your reliability objectives. From prediction analyses, to complex system modeling, to FMEA and FRACAS processes, Relex reliability software provides a complete tool set for all your reliability needs.

Relex Is the Name to Trust for Reliability Engineering Tools

Since 1986, Relex has been the software of choice for reliability excellence. With thousands of users in a wide range of industries around the globe, Relex has earned the trust of reliability professionals. From reliability analysis software, to training, service, and support, Relex Software is the name to trust for all your reliability needs.

Check out the tools trusted by reliability professionals worldwide. Go to **reliability.relex.com** to download our free trial version or register for a free interactive webinar. Or you can call us today at **724.836.8800** to get started.

Relex®
excellence in reliability

reliability.relex.com

The DTIC Total Electronic Migration System (TEMS): Providing Real-Time Access to Scientific and Technical Information...

Register or log in at https://tems-iac.dtic.mil/...

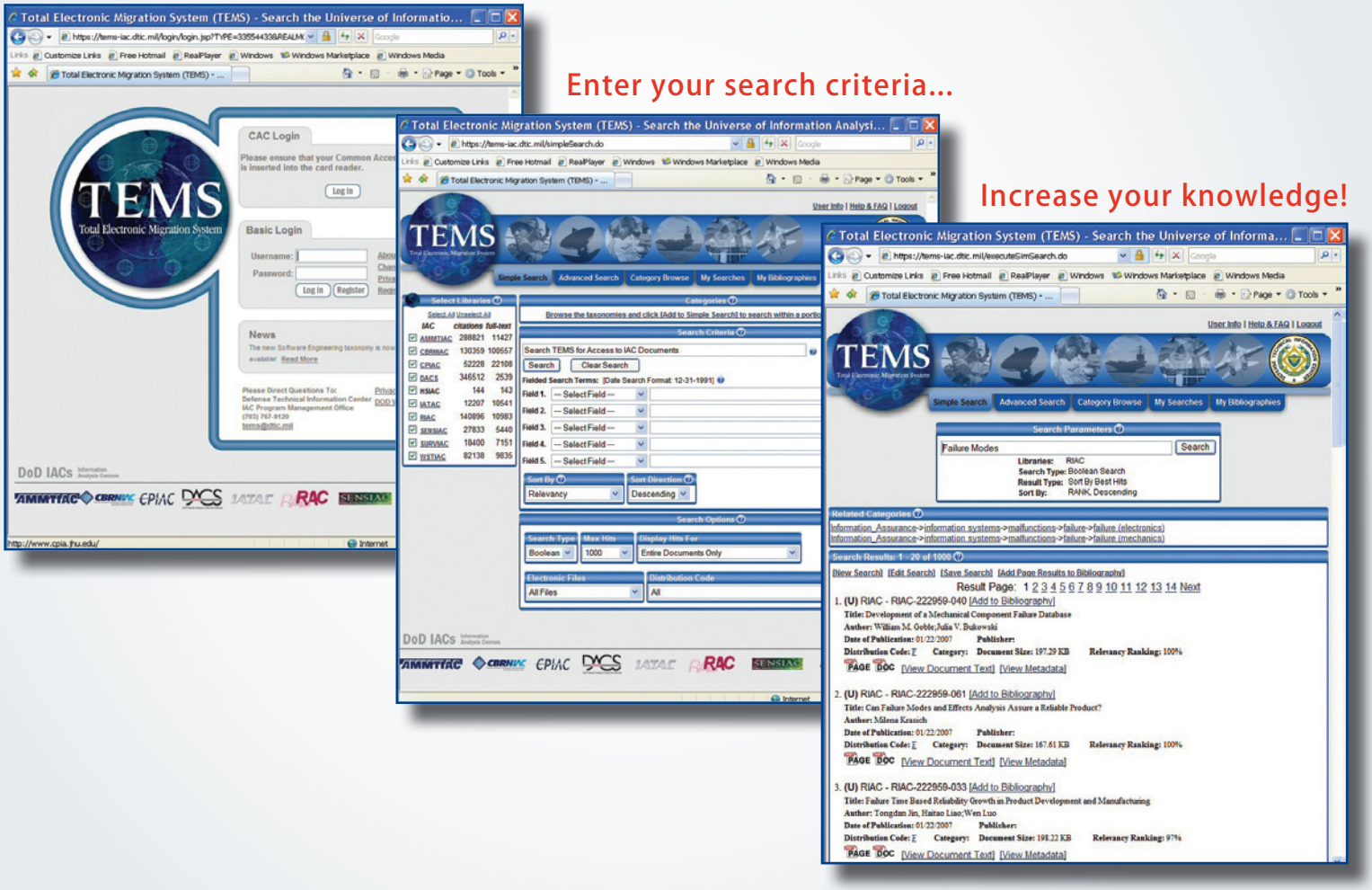

THE JOURNAL OF THE RELIABILITY INFORMATION ANALYSIS CENTER // FOURTH QUARTER - 2008

The Journal of the Reliability Information Analysis Center is published quarterly by the Reliability Information Analysis Center (RIAC). The RIAC is a DoD Information Analysis Center (IAC) sponsored by the Defense Technical Information Center (DTIC) and operated by a team led by Wyle Laboratories, and including Quanterion Solutions Incorporated, the Center for Risk and Reliability at the University of Maryland, the Penn State University Applied Research Lab (ARL) and the State University of New York Institute of Technology (SUNYIT).

The Reliability Information Analysis Center
6000 Flanagan Road
Suite 3
Utica, NY 13502-1348
Toll Free: 877.363.RIAC (7422)
P 315.351.4200 // FAX 315.351.4209
inquiry@theRIAC.org
http://theRIAC.org

RIAC Journal Editor, David Nicholls
Toll Free: 877.363.RIAC (7422)
P 315.351.4202 // FAX 315.351.4209
dnicholls@theRIAC.org

Richard Hyle
RIAC Contracting Officer's Representative,
Air Force Research Laboratory
P 315.330.4857 // FAX 315.330.7647
richard.hyle@rl.af.mil

Joseph Hazeltine
RIAC Director,
Technical Area Task (TAT) Manager
P 256.716.4390 // FAX 256.721.0144
joseph.hazeltine@wyle.com

Preston MacDiarmid
RIAC Technical Director
Toll Free 877.808.0097
P 315.732.0097 // FAX 315.732.3261
pmacdiarmid@quanterion.com

Valerie Hayes
RIAC Deputy Director TATs/SAs
P 301.863.4301 // FAX 301.863.4281
valerie.hayes@wyle.com

David Nicholls
RIAC Operations Manager
Toll Free 877.363.RIAC (7422)
P 315.351.4202 // FAX 315.351.4209
dnicholls@theRIAC.org

David Mahar
RIAC Webmaster,
Software & Database Manager
Toll Free 877.808.0097
P 315.732.0097 // FAX 315.732.3261
dmahar@theRIAC.org

Patricia Smalley
RIAC Training Coordinator
Toll Free 877.363.RIAC (7422)
P 315.351.4200 // FAX 315.351.4209
psmalley@theRIAC.org

Affordable tools for improving reliability…

QuART PRO
Quanterion Automated Reliability Toolkit V2.0

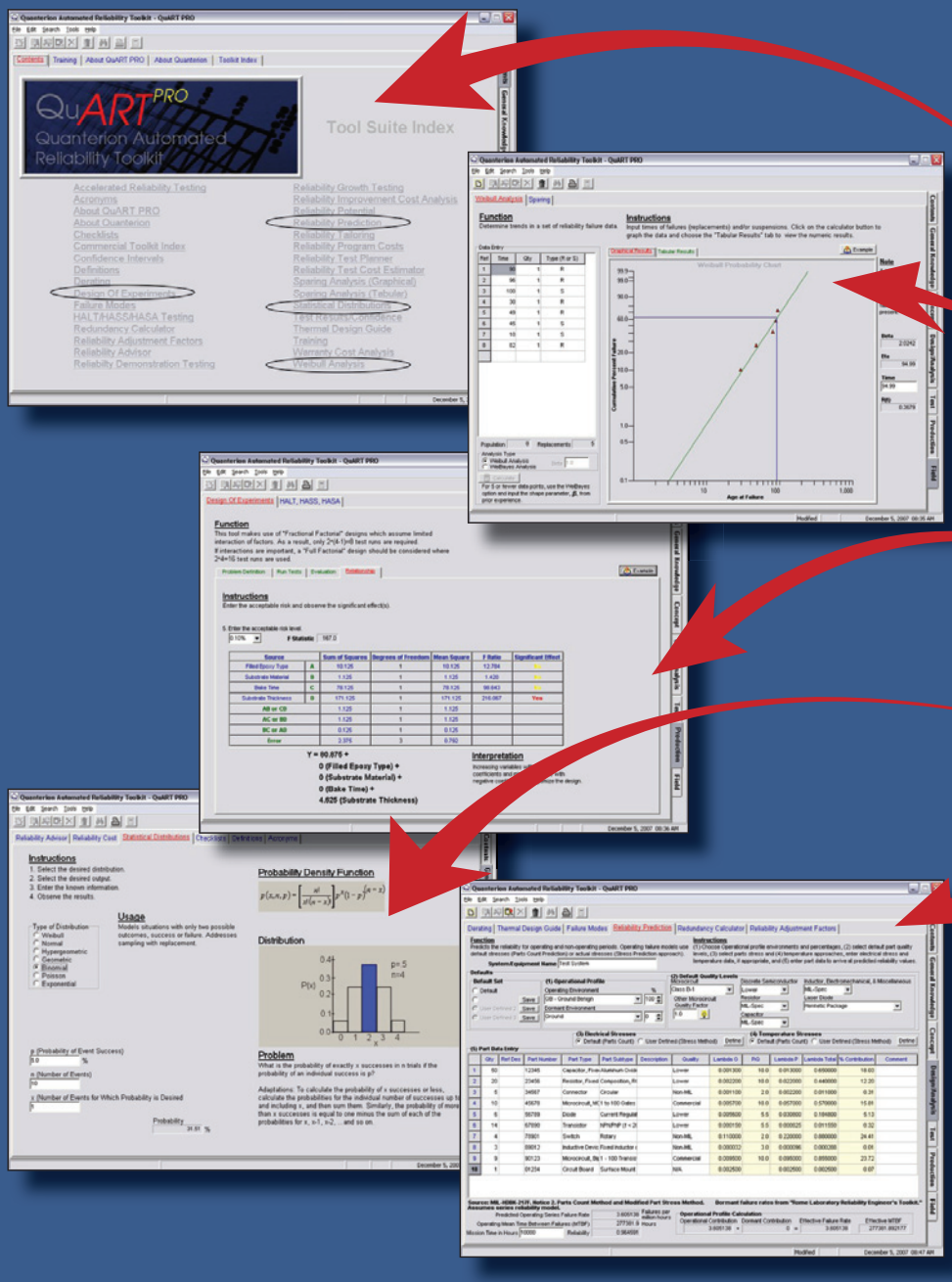

Downloadable for Only $189

- More Than 20 Reliability Tools and Advisors
- Weibull Analysis- to Understand the Nature of Failure Trends
- Design of Experiments- to Understand the Effects on Reliability
- Statistical Distributions- to Understand the Variability of Events
- Reliability Prediction- to Tradeoff Design Alternatives

QUANTERION SOLUTIONS INCORPORATED

quanterion.com

(315)-732-0097/(877) 808-0097

Quanterion Solutions is a team member in the operation of the Reliability Information Analysis Center (RIAC)

THE RIAC 217PLUS™ SOFTWARE FAILURE RATE MODEL

David Nicholls, RIAC (Quanterion Solutions Incorporated)

In this edition of the Journal, we present the 217Plus™ software model in its entirety. The model form is different than those for the hardware component models previously described [References 1 through 7]. Its development is discussed in more detail in Reference 8. A brief example will be provided at the end of the article.

Development of the 217Plus™ Software Failure Rate Model

Modern systems (and systems of systems) typically depend on significant amounts of software. Therefore, for a reliability assessment tool to be complete, it must include provisions for the estimation of software reliability. Many of the existing software reliability models are estimation models that require empirical test data. In many cases, data is simply not available at a point in time when a reliability estimate of a system is needed. Therefore, it was necessary to develop a predictive software reliability model that does not require empirical data. Like the 217Plus™ component models, the technique must be based on readily accessible data and information.

Like the hardware component models presented previously (and included in their entirety in Reference 9), the premise of the software model is that the inherent fault density of software can be estimated as a function of the development processes. However, in the software model, a separate process grading criteria is not included. Rather, due to its acceptance within the industry, the SEI (Software Engineering Institute) Capability Maturity Model (CMM) was used for this purpose. Once the inherent fault density is estimated as a function of the achieved CMM level, it is converted to a failure rate based on the defined operational profile of the software.

The 217Plus™ software reliability growth characteristics are modeled in a manner similar to that of hardware. For example, the potential for software reliability growth is assessed and the likely failure rate impact as a function of time is estimated. Both the growth rate and the stabilization time are estimated for this purpose. The default time for items to plateau and their residual fault content to stabilize is typically 48 months following its initial release. Subsequent item releases, such as a new software version, typically take 24 months to stabilize. In the case of software, this reliability growth is a function of the organization that will perform the field maintenance, which may be different than the development organization.

The user must assess the SEI Capability Maturity Model Level of the process developing the code. This assessment should be based upon the actual SEI assessment, if that exists. Lacking a SEI assessment of the development facility, one can use the Safety Level of the Software Level that the software is being developed to meet, or the ISO 9000 facility rating. If none of the cited process ratings exist, then review the SEI CMM Level requirements to determine and apply the CMM Level that most reasonably fits this item. (It should be noted that the SEI has since updated their CMM, defining it as CMM-Integrated (or CMMI). The structured version of the CMMI retains the same five-level format as its predecessor, so the basic methodology for using the 217Plus™ software reliability prediction model remains valid.)

The "Defect Stabilization Level" values should only be used if the organization that is maintaining the software has processes in place that will improve the reliability of the delivered code after faults are identified. If such growth processes are not in place, then the stabilization level that should be used is 100%. Also, the CMM level used for determining the defect stabilization level should be that of the maintaining organization, which could be different from that of the development organization.

Determining the Reliability Growth Coefficient

The software reliability grows as the fault content decreases exponentially over time, which results from the number of faults experienced and removed in the code, and is proportional to the total number of faults in the code. The empirical evidence shows program faults are discovered and removed exponentially over time as follows:

$$F(t) = F_0 e^{-kt}$$

where,

$F(t)$ = Current number of faults remaining in the code after calendar time, t
F_o = Initial number of faults in the code at delivery
k = Reliability growth constant
t = Calendar time in months

Taking the natural log of both sides of this equation yields:

$$k = \left(\frac{1}{t}\right)\ln\left(\frac{F_0}{F(t)}\right)$$

The reliability growth constant, k, is determined such that the latent fault content drops to its stabilization level or proportion of the initial faults as determined by the defect stabilization level, after the stabilization time. For example, for CMM Level 1 code, the constant "k" is determined by solving this equation for F(t) dropping to 10% at t = 48 months. Then (F_o/F(t)) = 10, and k = 0.048 per month.

Converting Fault Density to An Operational Failure Rate

The fault removal curve equation represents reliability growth. For purposes of estimating the operational failure rate of the fielded code, one can apply a linear, piece-wise approximation to the exponential curve. This simplifies calculation of an average failure rate over the time interval. The number of faults found and removed is indicative of the failure rate of the software. That is, it usually takes a failure to uncover an underlying fault in the software. The more failures that occur, the more underlying faults there are revealed in the code. The software failure rate, λ, is related to the number of underlying faults as follows:

$$\lambda(t) = \frac{F(t_2) - F(t_1)}{t_2 - t_1}$$

Adding a constant of proportionality, FER,

$$\lambda(t) = FER \times \frac{F(t_2) - F(t_1)}{t_2 - t_1}$$

where "FER" is the Fault Expansion Ratio, a factor which accounts for the elements summarized in Table 1.

The faults contained in the FER version of the software failure rate equation are generally classified into four severity classes (1, 2, 3, 4). Severity 1 usually implies a failure that is disabling to the application. Severity 2 implies a serious, but not catastrophic, disruption of work. Severity 3 and 4 are much less severe failures that would usually be considered just annoyances. A value between 0.0 and 1.0 would represent the percentage of all faults that would be disruptive and considered serious by the customer.

217Plus™ Software Failure Rate Model

The basic form of the 217Plus™ Software Model [Reference 9] is:

$$\lambda_{SW} = \left(\frac{F_{t_i-1} - F_{ti}}{730}\right)(DC \times FL \times FA \times AS) \times 10^6$$

where,

λ_{SW} = Predicted software failure rate at month t_i (in failures per million calendar hours)

F_{t_i} = Number of faults remaining at time t_i

$$F_{t_i} = F_0 e^{-kt_i}$$

F_0 is the initial defect density, and is calculated as:

$$F_0 = KSLOC \times FD$$

KSLOC = Lines of source code (in thousands)

FD = Fault Density (default from Table 3)

Table 1: Elements of the Fault Expansion Ratio (FER)

Parameter Symbol	Name	Description	Default
FL	Fault Latency	Average number of times a failure is expected to reoccur before its underlying fault is corrected	2.0 (dimensionless number)
FA	Fault Activation	Fraction (in decimal form) of population exhibiting fault activation	1.0 (100%)
AS	Average % Severity	Fraction (in decimal form) of faults that are disruptive, or critical, to the customer	0.5 (50%)
DC	Duty cycle	Fraction of calendar time the software is in operation (in decimal form)	Operational profile duty cycle

continued on next page ›››

continued from page 19

k is the growth rate, and is:

$$k = \frac{\ln\left(\frac{1}{DSL}\right)}{t_s}$$

t_i = Time (in months) after deployment
t_s = Time (in months) to software stabilization (default from Table 2)
DSL = Defect Stabilization Level (default from Table 3)
F_{t_i-1} = Number of faults remaining at time, t_i-1

$$F_{t_i-1} = F_0 e^{-k(t_i-1)}$$

The model parameters, and their symbol, description, and default value, are summarized in Table 2. Table 3

Whenever actual company experience exists, it should be substituted for the heuristic 217Plus™ reliability profiles summarized in Table 4. Use your own recent item history if your company has determined the latent defect density of its systems or products.

Example Calculation

A new release of a software program for an entertainment system used on a commercial aircraft for international and transcontinental travel has been used in the field for thirty-six (36) months. The software program is implemented using 245,500 lines of source code (i.e., comment lines and other non-executable code are not counted). The organization that developed the software code, and the organization that supports/maintains it, have each been certified as being SSEI CMM Level 3 compliant. Through the collection and analysis of its own data, a number of measurements and metrics have been established. An analysis of the software operational profile has determined that the software program is exercised approximately 70% of the calendar time each year (the software is non-operational during taxi, takeoff and landing, and when the aircraft is out of service for maintenance or normal downtime). The company has also determined that, on average, a failure reoccurs 2.6 times before the underlying fault is correctly identified and corrected. To date, 5% of the fielded systems containing this new software-have experienced faults resulting in intermittent system interruptions lasting between 5 and 30 seconds. The fraction of these faults that are considered annoying to the customer is around 10%, as they occur primarily during routine "canned" safety instructions. At the time the new software was "shipped", the company measured the fault density as 2.1 remaining defects per thousand lines of source code. Finally, based on its SEI CMM Level 3 certification, the company accepts a default value of 0.05 as its Defect Stabilization Level.

The failure rate equation for software [Reference 9] is:

$$\lambda_{SW} = \left(\frac{F_{t_i-1} - F_{ti}}{730}\right)(DC \times FL \times FA \times AS) \times 10^6$$

The initial defect density, F_0, is calculated as $F_0 = 245.5 * 2.1 = 515.55$ defects based on 245,500 lines of source code and FD = 2.1 (given).

Table 2: Parameters Used in the 217Plus™ Software Model

Parameter Symbol	Name	Description	Default
KSLOC	Lines of Source Code (in thousands)	Lines of source code (in thousands), not including comments, i.e., size of the software	None
FD	Fault Density	Initial quality as measured by fault density at item shipment	Table 3
FL	Fault Latency	Average number of times a failure is expected to reoccur before its underlying fault is corrected	2.0 (dimensionless number)
FA	Fault Activation	Fraction (in decimal form) of population exhibiting fault activation	1.0 (100%)
AS	Average % Severity	Fraction (in decimal form) of faults that are disruptive, or critical, to the customer	0.5 (50%)
ts	Time to Stabilization		48 (months) for initial software release. However, this value should be changed to 24 (months) for subsequent software releases.
DSL	Defect Stabilization Level	The level at which the software failure rate stabilizes relative to F0	Table 3
DC	Duty Cycle	Fraction of calendar time the software is in operation (in decimal form)	Operational profile duty cycle

Table 3: Default Values of Defect Density (FD) and Defect Stabilization Level (DSL)

SEI'S CMM Level	Initial Design Defect Density (FD) (Defects per 1000 lines of source code, for all severities)	Defect Stabilization Level (DSL)
5	0.5	0.01
4	1.0	0.03
3	2.0	0.05
2	3.0	0.07
1	5.0	0.10
Unrated	6.0	Not Estimated

Table 4: Default Operating Profile Values

Equipment Type	Operating Profile	
	Duty Cycles	Cycling Rate (Cycles/yr)
Automotive	5	1000
Commercial Aircraft	25	2982
Computer	80	1491
Consumer	30	368
Emergency Power	10	50
Industrial	80	184
Military Aircraft	25	1008
Military Ground	45	263
Telecommunications	80	368

The growth rate factor, *k*, is calculated to be:

$$k = \frac{\ln\left(\frac{1}{0.05}\right)}{48} = 0.0624$$

where,

DSL = 0.05, based on SEI CMM Level 3 certification (from Table 3)

t_s = 48, based on an initial software release (from Table 2)

The number of faults remaining at 36 months, F_{36}, is:

$$F_{36} = 515.55e^{-(0.06241)(36)} = 54.51$$

The number of faults remaining at 35 months, F_{35}, is:

$$F_{35} = 515.55e^{-(0.06241)(35)} = 58.02$$

DC = 0.70 (given as 70%)

FL = 2.60 (given)

FA = 0.05 (given as 5%)

AS = 0.10 (given as 10%)

$$\lambda_{SW} = \left(\frac{58.02 - 54.51}{730}\right)(0.70)(2.60)(0.05)(0.10)\left(10^6\right) = 43.76$$

λ_{SW} = 43.76 f/10^6 calendar hours

References:

1. "An Introduction to the RIAC 217Plus™ Component Failure Rate Models", Journal of the Reliability Information Analysis Center, First Quarter 2007, available for PDF download from the RIAC at http://theRIAC.org
2. "The 217Plus™ Capacitor and Diode Failure Rate Models", Journal of the Reliability Information Analysis Center, Second Quarter 2007, available for PDF download from the RIAC at http://theRIAC.org
3. "The 217Plus™ Integrated Circuit and Inductor Failure Rate Models", Journal of the Reliability Information Analysis Center, Third Quarter 2007, available for PDF download from the RIAC at http://theRIAC.org
4. "The 217Plus™ Transformer and Optoelectronic Device Failure Rate Models", Journal of the Reliability Information Analysis Center, Fourth Quarter 2007, available for PDF download from the RIAC at http://theRIAC.org
5. "The 217Plus™ Switch and Relay Failure Rate Models", Journal of the Reliability Information Analysis Center, First Quarter 2008, available for PDF download from the RIAC at http://theRIAC.org
6. "The 217Plus™ Connector and Resistor Failure Rate Models", Journal of the Reliability Information Analysis Center, Second Quarter 2008, available for PDF download from the RIAC at http://theRIAC.org
7. "The 217Plus™ Transistor and Thyristor Failure Rate Models", Journal of the Reliability Information Analysis Center, Third Quarter 2008, available for PDF download from the RIAC at http://theRIAC.org
8. Denson, W.K. and Keene, S., "New System Reliability Assessment Methodology", Reliability Analysis Center, RAC Project #A06839, March 1997
9. Denson, W.K., "Handbook of 217Plus™ Reliability Prediction Models", Reliability Information Analysis Center (RIAC), 26 May 2006, ISBN 1-933904-02-X
10. "An Overview of the 217Plus™ System Reliability Assessment Methodology", Journal of the Reliability Information Analysis Center, Fourth Quarter 2006, available for

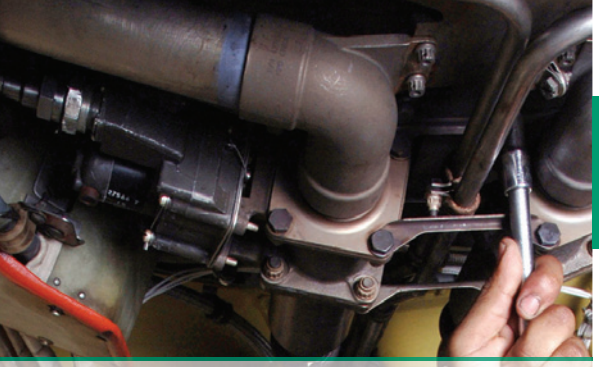

Introduction to Maintainability Engineering

On-Line Training Course

Course Description:

This course was developed by the RIAC as an introduction to maintainability engineering concepts and practices. It begins with a brief overview of the RIAC, and because maintenance demand is driven by system reliability, provides an overview of basic reliability engineering concepts before proceeding into the core maintainability topics.

Section 3 begins the core content by covering basic maintainability concepts and definitions, the need for maintainable systems and the elements of a comprehensive maintainability program.

Section 4 covers the basic mathematical foundations of maintainability by describing various probability distributions that are commonly used to model system maintainability.

Section 5 describes establishing maintainability requirements at the system level as well as at lower levels of design. These include establishing quantitative requirements, such as mean time to repair (MTTR), as well as techniques such as quality function deployment (QDF) that are used to ensure user requirements are met.

Section 6 delves into maintainability design techniques such as allocations, predictions, human engineering and standardization.

Section 7 covers maintainability verification approaches, including inspection, analytical methods and testing.

Section 8 describes trending methods to track and improve maintainability over time and

Section 9 discusses ensuring maintainability is not degraded by production decisions.

Section 10 provides a review and wrap-up of the course.

The course also includes two quizzes to reinforce the concepts covered.

Features & Benefits:

- 3 Days of live recorded feed including quizzes and demos, totaling over 14 Hours
- Synchronized PowerPoint presentations with video for maximum learning content
- On-Line training lets you learn at your own pace, anywhere, anytime, and save lots of money on travel expenses

View the online demo at: http://theRIAC.org

*Paid advertising appears on pages 14, 15, 17, 23, 26 and 27.

• Quantitative Risk Assessment • Reliability
• Availability • Maintainability • Safety

Reliability and Risk Solutions

Software Tools, Support, Training & Consulting

ITEM QRAS

- NASA© Sponsored Project
- Scenario-Based Risk Modelling
- Event Sequence Diagrams
- Fault Tree Analysis
- System Level Risk Aggregation
- Risk Level Quantification
- Risk Contributor Ranking
- Binary Decision Diagrams

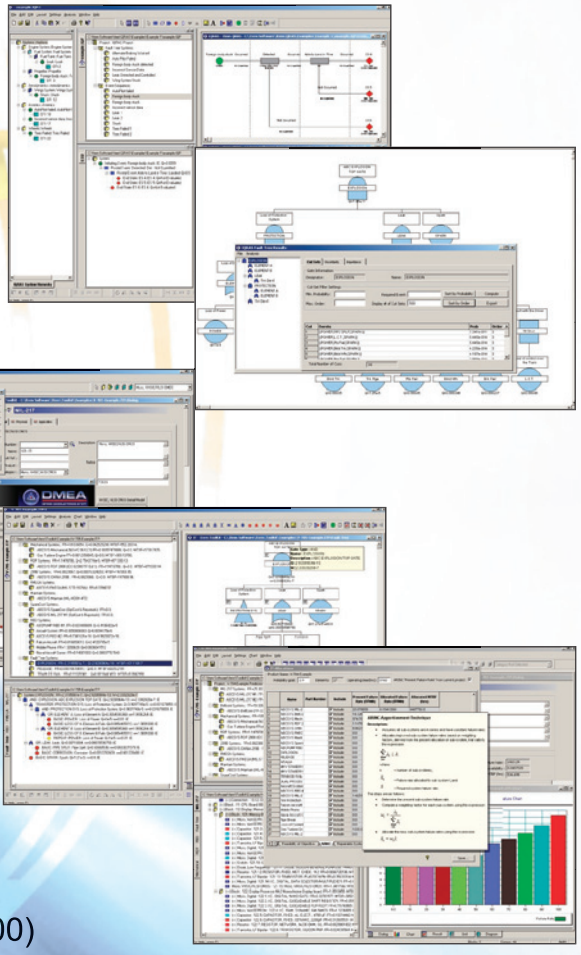

ITEM ToolKit

- Reliability Prediction
  - *MIL-HDBK-217*
  - *Bellcore/Telcordia*
  - *NSWC*
  - *IEC-62380*
  - *China 299B*
- Fault Tree Analysis
- Event Tree Analysis
- Markov Analysis
- Reliability Block Diagram
- Failure Mode Effect Analysis (FMEA, ISO 9000)
- Failure Mode Effect & Criticality Analysis (FMECA, MIL-STD-1629A)
- Failure Mode Effect & Diagnostics Analysis (FMEDA, IEC-61508)
- Maintainability Analysis
- Spares Scaling and Ranging

Over 7,000 satisfied customers worldwide.

item Software

Contact us now for a product evaluation CD or personalized web demonstration

USA Office: • Tel: +1 714.935.2900 • 866.761.ITEM (4836) • Fax: +1 714.935.2911
• Email: sales@itemsoft.com

UK Office: • Tel: +44 1489.885.085 • Fax: +44 1489.885.065
• Email: sales@itemuk.com

www.itemsoft.com **www.itemuk.com**

JANUARY

S	M	T	W	T	F	S
				1	2	3
4	5	6	7	8	9	10
11	12	13	14	15	16	17
18	19	20	21	22	23	24
25	26	27	28	29	30	31

2009 Annual Reliability and Maintainability Symposium // Fort Worth, TX

January 26, 2009 thru January 29, 2009
Contact: http://rams.org

2009 INCOSE International Workshop // San Francisco, CA

January 31, 2009 thru February 3, 2009
Contact: Karin Moens // P 33 (0)5 61 35 31 08 // F 33 (0)5 67 69 90 15 // karin.moens@askintlconference.com

FEBRUARY

S	M	T	W	T	F	S
1	2	3	4	5	6	7
8	9	10	11	12	13	14
15	16	17	18	19	20	21
22	23	24	25	26	27	28

2nd Annual Oil & Gas Pipeline Maintenance and Reliability // Vienna, Austria

February 10, 2009 thru February 12, 2009
Contact: Jacob Fleming // P +421 257 272 131 // F +421 253 632 370 // events@jacobfleming.com
F: +421 253 632 370
E: events@jacobfleming.com

MARCH

S	M	T	W	T	F	S
1	2	3	4	5	6	7
8	9	10	11	12	13	14
15	16	17	18	19	20	21
22	23	24	25	26	27	28
29	30	31				

25th Annual National Test and Evaluation National Conference // Atlantic City, NJ

March 2, 2009 thru March 5, 2009
Contact: Emily Agnew // P 703.247.2566 // eagnew@ndia.org

RIAC Open Training Program // San Diego, CA

March 10, 2009 thru March 12, 2009
Contact: Pat Smalley, Reliability Information Analysis Center // P 877.363.7422 or 315.351.4200 // F 315.351.4209 // psmalley@theRIAC.org

Performance-Based Logistics 2009 // Washington, DC

March 16, 2009 thru March 19, 2009
Contact: Institute for Defense And Government Advancement // P 800 882 8684 or 646 378 6026 // F 646 378 6025 // info@iqpc.com

Human Systems Integration (HSI) Symposium 2009 // Annapolis, MD

March 17, 2009 thru March 19, 2009
Contact: American Society of Naval Engineers (ASNE) // P 703.836.6727 // membership@navalengineers.org

Reliability Centered Maintenance Managers' Forum (RCM2009) // Daytona Beach, FL

March 23, 2009 thru March 26, 2009
Contact: NetExpressUSA Inc. // P 888.575.1245 or 239.340.6749 // F 309.423.7234 // info@netexpressusa.com

APRIL

S	M	T	W	T	F	S
			1	2	3	4
5	6	7	8	9	10	11
12	13	14	15	16	17	18
19	20	21	22	23	24	25
26	27	28	29	30		

21st Annual Systems & Software Technology Conference (SSTC) // Salt Lake City, UT

April 20, 2009 thru April 23, 2009
Contact: General Registration // P 435.797.0423 // F 435.797.0036 // sstc-info@ext.usu.edu

2009 IEEE International Reliability Physics Symposium // Montreal, Quebec, Canada

April 26, 2009 thru April 30, 2009
Contact: http://www.irps.org

Please fax completed survey to
315.351.4209 – ATTN: Journal Editor

RIAC JOURNAL SURVEY

FOURTH QUARTER - 2008

Journal Format ☑ Hard Copy ☐ Web Download

How satisfied are you with the **content** (article technical quality) in *this issue* of the Journal?

☐ Very Satisfied ☐ Satisfied ☐ Neutral ☐ Dissatisfied ☐ Very Dissatisfied

How satisfied are you with the **appearance** (layout, readability) of *this issue* of the Journal?

☐ Very Satisfied ☐ Satisfied ☐ Neutral ☐ Dissatisfied ☐ Very Dissatisfied

How satisfied are you with the **overall quality** of *this issue* of the Journal (compared to similar magazines, newsletters, etc.)?

☐ Very Satisfied ☐ Satisfied ☐ Neutral ☐ Dissatisfied ☐ Very Dissatisfied

How did you become **aware** of *this issue* of the Journal?

☐ Subscribe ☐ Colleague ☐ Library ☐ RIAC Website ☐ RIAC Email ☐ Conference/Trade Show

Would you **recommend** the RIAC Journal to a colleague?

☐ Definitely ☐ Probably ☐ Not Sure ☐ Probably Not ☐ Definitely Not

Please suggest general **changes / improvements** to the RIAC Journal that would improve your level of satisfaction:

Please suggest further **topics** for the RIAC Journal that might help it to better meet your needs:

Overall satisfaction

☐ Very Satisfied (5) ☐ Satisfied (4) ☐ Neutral (3) ☐ Dissatisfied (2) ☐ Very Dissatisfied (1)

CONTACT INFORMATION (OPTIONAL)

Name Position/Title

Organization Office Symbol

Address City State Zip

Country Email

Phone Fax

My Organization is: ☐ Army ☐ Navy ☐ Air Force ☐ Other DoD/Government ☐ Industry ☐ Academic ☐ Other

I need help with a reliability, maintainability, quality, supportability, or interoperability problem. ☐ Please contact me

RIAC TRAINING

RELIABILITY INFORMATION ANALYSIS CENTER

Patricia Smalley
RIAC Training Coordinator
Toll Free 877.363.RIAC (7422)
P 315.351.4200 // F 315.351.4209
psmalley@theRIAC.org
http://theRIAC.org/Training

RIAC Training in San Diego, CA // March 10 - 12, 2009

Choose From

Reliability 101
Seymour Morris, Quanterion Solutions

$1,295.00 per attendee

Mechanical Design Reliability
Ned H. Criscimagna, Criscimagna Consulting

$1,295.00 per attendee

Reliability Centered Maintenance (RCM) for the Analyst
Roger Collard, CMRP

$1,295.00 per attendee

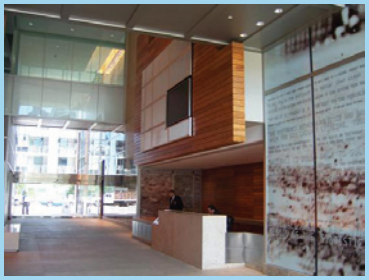

Hosted at the San Diego Training and Conference Center

For more information and to register visit
http://theRIAC.org or call 877.363.7422

*Discounts apply to multiple registrations from an organization. Please contact the RIAC for details.

**Course instructors are subject to change.

Reducing Program Risk Through Independent Testing for 57 Years

Wyle Laboratories, Inc. has provided trusted agent test and evaluation services for more than 57 years. Throughout that period, Wyle has provided quality data that has been key to reducing program risk, resulting in increased system effectiveness for the warfighter. From component testing in the early development phases to independent test engineering services s u p p o rting the operational test phase, through ongoing life cycle evaluation and support, Wyle's exceptional services have been unparalleled across the test continuum.

→ TEST CONTINUUM →

Advanced Concept Technology Demonstration	Advanced Technology Demonstration	Operational Assessment	Contractor Test and Evaluation	Developmental Test and Evaluation	Initial Operational Test and Evaluation	Live Fire Test and Evaluation	Operational Assessment	Initial Operational Test and Evaluation	Follow-on Operation Test and Evaluation	Joint Test and Evaluation

Through its dedication to provide high level engineering expertise at all stages of the testing process, Wyle today significantly improves the operational performance, effectiveness, and suitability of sea, air, land and space systems and platforms. With capability, capacity and commitment, Wyle reduces program risk, getting the very best systems fielded for the warfighter.

wyle laboratories

www.wylelabs.com e-mail: service@wylelabs.com

THE RIAC ONLINE

▷▷▷ The RIAC's "Desk Reference" is a Virtual Knowledge base of reliability know-how on best practices, analyses and test approaches.

▷▷▷ Save time and money at the RIAC's online store where you can browse, order, and immediately download electronic versions of most of the RIAC's products.

- Online Product Store
- RMQSI Library
- Technical Answers
- The RIAC Journal
- Upcoming Training Courses
- What's New at RIAC

Reliability Information Analysis Center
6000 Flanagan Road | Suite 3 | Utica, NY 13502-1348

PRSRT STD
U.S. Postage
Paid
Utica, NY
Permit #566